substance: boron compounds with lanthanides
property: properties of lanthanide hexaborides: CeB_6

Structure, chemical bond

There are three phases in the temperature versus magnetic field diagram [83T2]); (i) high temperature phase characterized by a pronounced Kondo effect [80K, 80T], (ii) an intermediate phase, in which two kinds of hyperfine fields are assumed to be due to an ordering of the higher order multipole moments (antiquadrupolar ordering) of Ce ions, while the the magnetic dipole moment has only the uniform component [83T2], (iii) low-temperature phase with a long-range magnetic order [82B].

Magnetic field – temperature phase diagram at ambient pressure in Fig. 1 [85B]. For phase diagrams at higher pressures see reference.

NMR study of CeB_6, temperature dependence of the nuclear relaxation time and correlation time of Ce moments in [83T2].

NMR study of the spin structure in CeB_6 [83T1].

Electronic properties

Calculation of the electronic band structure (FLAPW method) and positron annihilation in CeB_6 (compared with LaB_6) [89K].

Electronic band structure in Fig. 2 [89K].

energy gap

E_g	45 meV	T =13...53 K	electron-tunneling	98A

Electron-tunneling studies compared with SmB_6, EuB_6, SrB_6 in [98A].

CeB_6 possesses a magnetic moment like SmB_6 and EuB_6 but in contrast to SrB_6 [98A].

Richardson plot for CeB_6 (and LaB_6) with excess B ($CeB_{6.07}$ and $LaB_{6.06}$) compared with pure crystals in Fig. 3 [96O1].

Lattice properties

anisotropic thermal parameters for the B atom
(in Å^2)

U_{11}	0.00308	T = 100 K	from diagram in [93T]	85S1
	0.00312	T = 300 K		
U_{22}	0.0045	T = 100 K		
	0.0049	T = 300 K		

elastic constants
(in 10^{11} dyn cm^{-2})

c_{11}	40.30		calculated (one specific model)	85T
	40.6		experimental	
c_{12}	–8.59		calculated	83G
	–9.3		experimental	
c_{44}	9.91		calculated	85S2
	7.8		experimental	

Optical properties

Differences between LaB_6 and CeB_6 by means of spectroscopic ellipsometry [86V].

Further properties

Entropy in [86B].

Search for rugged, efficient photocathode materials (CeB_6 and LaB_6) [92B].

melting point

T_m	2550 °C			96G

Debye temperature

Θ_D	381 K	T = 300 K		85S2

For Einstein temperatures of metal hexaborides, see Fig. 4.

microhardness

H_K	2250 kg mm^{-2}	T = 300 K	cube, average value; load 50 g	96G
	2150 kg mm^{-2}		cube, average value; load 100 g	

High temperature hardness of single crystals of LaB_6, CeB_6, PrB_6, NdB_6 and SmB_6 [99O].

Evaporation rates of pure CeB_6 and CeB_6 with excess B compared with corresponding LaB_6 crystals in Fig. 5 [96O1].

Thermionic emission properties of CeB_6 (compared with LaB_6) in [96O1, 96O2].

Susceptibility vs. magnetic field at different T in Fig. 6 [85B].

Magnetization vs. temperature in Fig. 7 [80K].

Susceptibility vs. temperature in Fig. 8 [80K].

Pressure dependence of Néel and antiferroquadrupolar temperatures in Fig. 9 [85B].

References:

80K Kawakami, M., Kunii, S., Komatsubara, T., Kasuya, T.: Solid State Commun. 36 (1980) 435.

80T Takase, S., Kojima, K., Komatsubara, T., Kasuya, T.: Solid State Commun. 36 (1980) 461.

82B Burlet, P., Rossat-Mignod, J., Effantin, J.M., Kasuya, T.: J. Appl. Phys. 53 (1982) 2194.

83G Goto, T., Tamaki, A., Kunii, S., Nakajima, T., Fujimura, T., Kasuya, T., Komatsubara, T., Woods, S.B.: J. Magn. Magn. Mater. 31 (1983) 419.

83T1 Takigawa, M., Yasuoka, H., Tanaka, T., Ishizawa, Y.: J. Phys. Soc. Jpn. 3 (1983) 728.

83T2 Takigawa, M., Yasuoka, H., Tanaka, T., Ishizawa, Y., Kasaya, M., Kasuya, T.: J. Magn. Magn. Mater. 31-34 (1983) 391.

85B Brandt, N.B., Moshchalkov, V.V., Pashkevich, S.N., Vybornov, M.G., Semenov, M.V., Kolobyanina, T.N., Konovalova, E.S., Paderno, Yu.B.: Solid State Commun. 56 (1985) 937.

85S1 Sato, S.: J. Magn. Magn. Mater. 52 (1985) 310 (structural data of CeB_6).

85S2 Smith, H.G., Dolling, G., Kunii, S., Kasaya, M., Liu, B., Takegahara, K., Kasuya, T., Goto, T.: Solid State Commun. 53 (1985) 15.

85T Takegahara, K., Kasuya, : Solid State Commun. 53 (1985) 21.

86B Borovikova, M.S., Fesenko, V.V.: J. Less-Common Met. 117 (1986) 287. (Proc. 8th Int. Symp. Boron, Borides, Carbides, Nitrides and Rel. Compounds, Tbilisi, Oct. 8 - 12, 1984)

86V van der Heide, P.A.M., ten Cate, H.W., ten Dam, L.M., der Groot, R.A., de Vroomen, A.R.: J. Phys. F: Met. Phys. 16 (1986) 1617.

89K Kubo, Y., Asano, S.: Phys. Rev . B 39 (1989) 8822.

92B Bamford, D.J., Bakshi, M.H., Deacon, D.A.G.: Nucl. Instrum. Methods A 318 (1992) 377.

93T Trounov, V.A., Malyshec, A.L., Chernyshov, D.Yu., Korsukonva, M.M., Gurin, V.N., Aslanov, L.A., Chernychev, V.V.: J. Phys.: Condens. Matter 5 (1993) 2479.

94K Korsukova, M.M.: Proc. 11th Int. Symp. Boron, Borides and Rel. Compounds, Tsukuba, Japan, August 22 - 26, 1993, Jpn. J. Appl. Phys. Series 10 (1994), p. 15.

96G Gurin, V.N., Derkachenko, L.I., Korsukova, M.M., Nikanorov, S.P., Jung, W., Müller, R.: Sov. Phys. Solid State 38 (1996) 1508.

96O1 Otani, S., Ishizawa, Y.: J. Alloys Compounds 245 (1996) L18.

96O2 Otani, S., Souda, R., Ishizawa, Y.: J. Ceram Soc. Jpn. Inter. Ed. 104 (1996) 1088.

98A Ambler, B., Fisk, Z., Sarrao, J.L., v. Molnar, S., Meisel, M.W., Sharifi, F.: Phys. Rev. B 57 (1998) 8747.

99O Otani, S., Nakagawa, H., Nishi, Y., Kieda, N.: J. Solid State Chem. (2000) (Proc. 13th Int. Symp. Boron, Borides and Rel. Compounds, Dinard, France, Sept. 1999).

99T Takahashi, Y., Ohshima, K., Okamura, F.P., Otani, S., Tanaka, T.: J. Phys. Soc. Jpn. 68 (1999) 2304.

Fig. 1.

CeB_6. Magnetic field vs. *T* phase diagram at ambient pressure [85B]. AFM: antiferromagnetic, PM: paramagnetic, AFQ: antiferroquadrupolar.

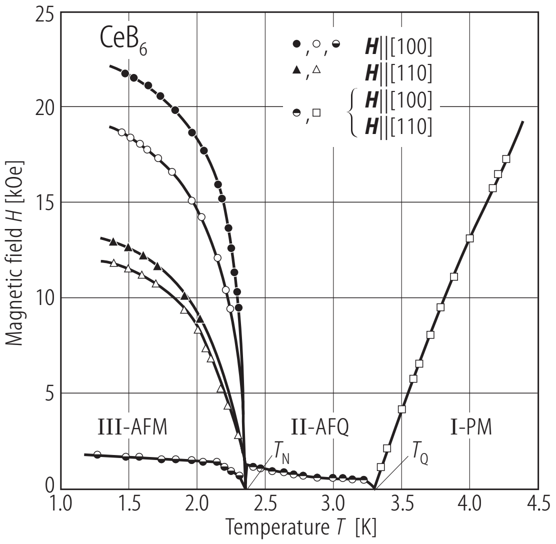

Fig. 2.

CeB_6. Calculated electronic band structure FLAPW (full-potential linearized augmented-plane-wave) method [89K]. Dashed line: Fermi level.

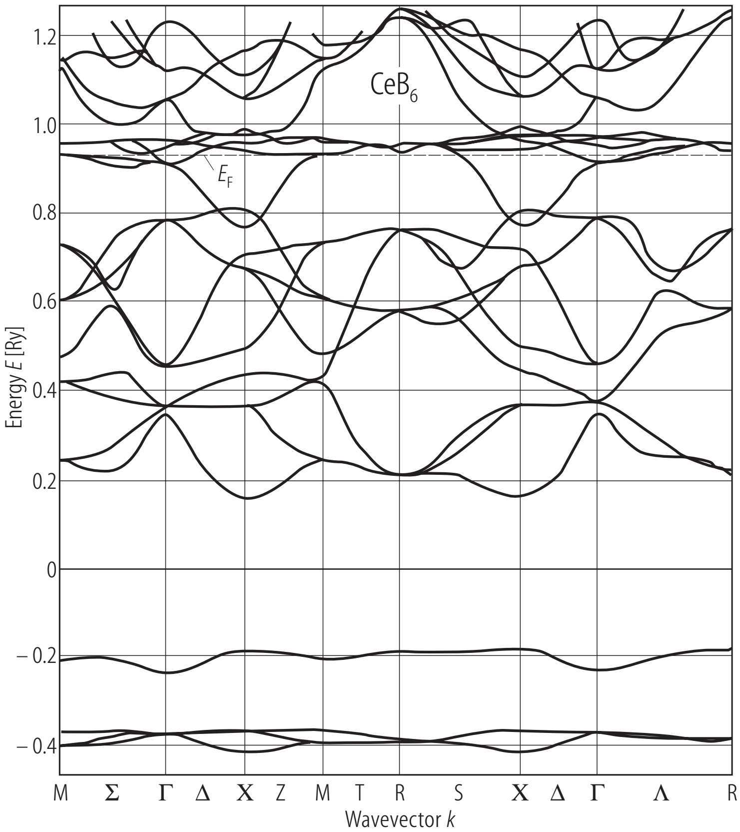

Fig. 3.

LaB_6, CeB_6. Richardson plots for LaB_6 and CeB_6 crystals with excess B compared with pure material [96O1]. Crystal diameter: 0.5 cm.

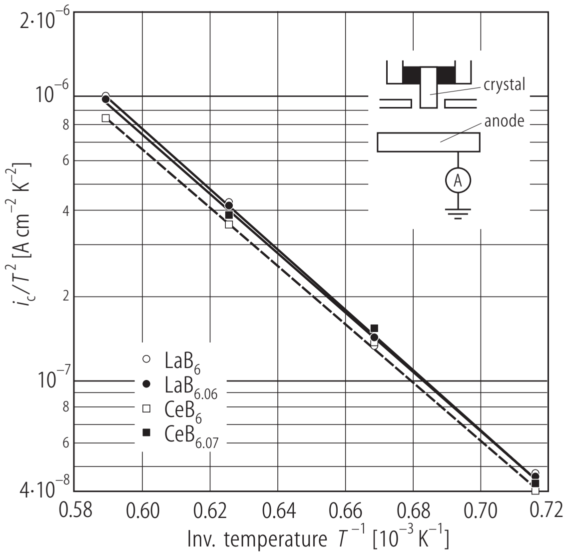

Fig. 4.

Metal hexaborides. Characteristic Einstein temperatures of the Ln atoms vs. atomic number of the Ln element; full circles [94K]; triangles [99T].

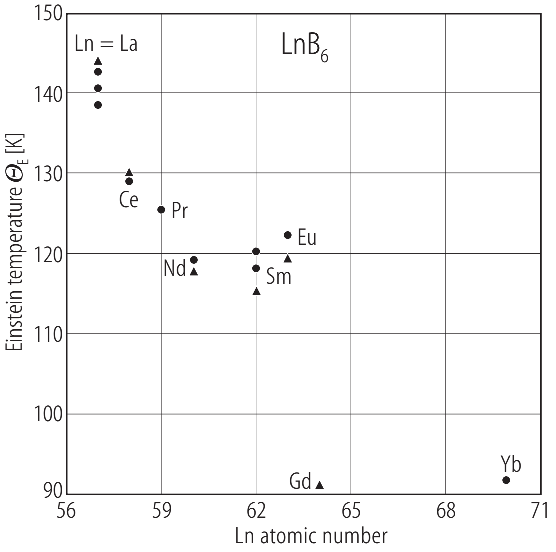

Fig. 5.

LaB_6, CeB_6 :B. Evaporation rate of pure LaB_6 and CeB_6 with excess B compared with the corresponding pure crystals [96O1].

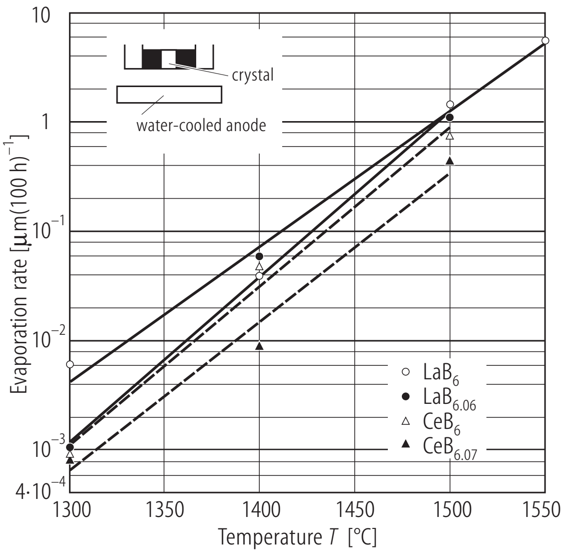

Fig. 6.

CeB_6.Magnetic susceptibility χ vs. magnetic field H in arbitrary units. Typical curves for specific temperature ranges. For the symbols at the peaks see Fig. 1 [85B].

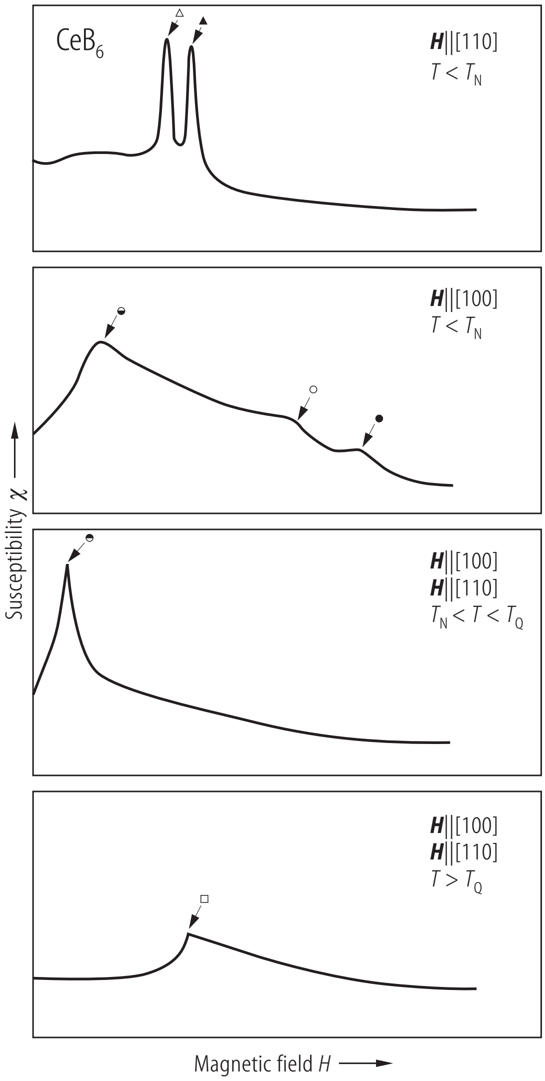

Fig. 7.

CeB_6. Specific magnetization in 750 Oe vs. *T*; solid circles, [100]; open circles, [110]; triangles, [111].[80K].

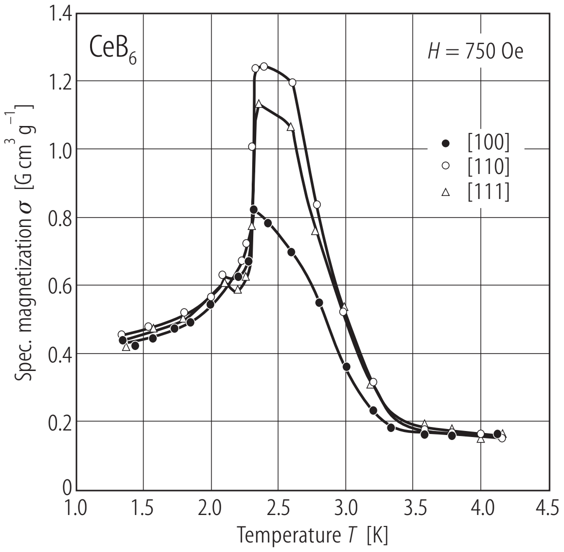

Fig. 8.

CeB_6. Inverse magnetic susceptibility $1/\chi_g$ (in CGS-emu) vs. *T*. Circles, experimental results; dotted line, calculated. [80K].

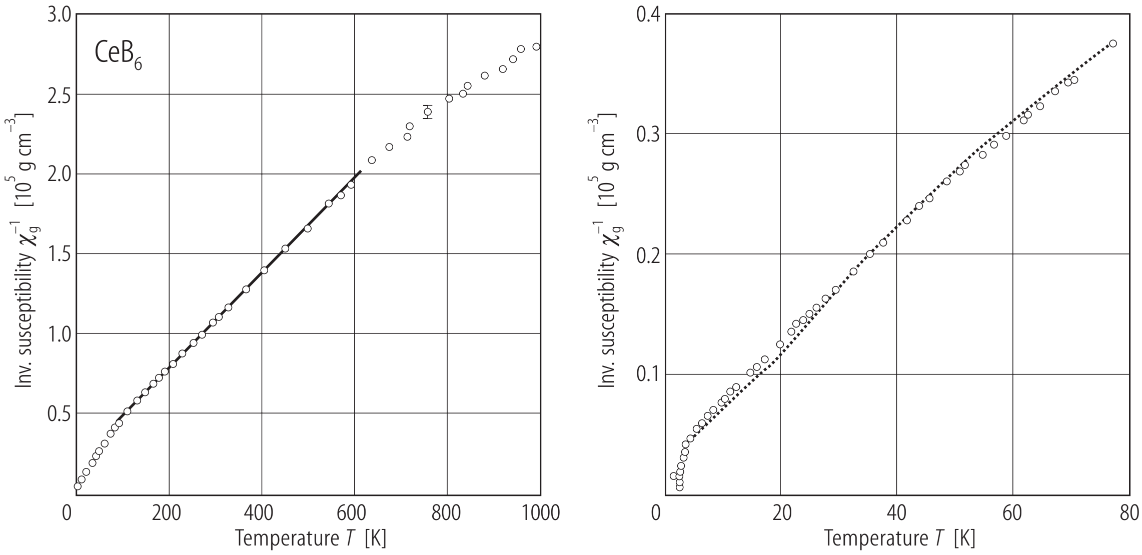

Fig. 9.

CeB_6. Néel temperature and antiferro-quadrupolar temperature vs. pressure [85B].